

Migration mechanisms of self-interstitial atoms and their clusters in Fe-Cr alloys

A molecular dynamics study

Dmitry Terentyev and Lorenzo Malerba

June, 2006

SCK•CEN
Boeretang 200
2400 Mol
Belgium

Eurotrans IP/DEMETRA

Migration mechanisms of self-interstitial atoms and their clusters in Fe-Cr alloys

A molecular dynamics study

Dmitry Terentyev and Lorenzo Malerba

May, 2006
Status: Unclassified
ISSN 1379-2407

SCK•CEN
Boeretang 200
2400 Mol
Belgium

Eurotrans IP/DEMETRA

© SCK•CEN
Belgian Nuclear Research Centre
Boeretang 200
2400 Mol
Belgium

Phone +32 14 33 21 11
Fax +32 14 31 50 21

<http://www.sckcen.be>

Contact:
Knowledge Centre
library@sckcen.be

RESTRICTED

All property rights and copyright are reserved. Any communication or reproduction of this document, and any communication or use of its content without explicit authorization is prohibited. Any infringement to this rule is illegal and entitles to claim damages from the infringer, without prejudice to any other right in case of granting a patent or registration in the field of intellectual property. SCK•CEN, Boeretang 200, 2400 Mol, Belgium.

Abstract

The mobility of self-interstitial atoms (SIAs) and their clusters in pure iron and iron-chromium alloys was studied by atomic scale modelling techniques. Molecular dynamics (MD) was used to simulate thermally activated motion, i.e. diffusion, and its mechanisms whereas molecular statics was used to estimate energies of interactions of SIA and SIA clusters with Cr-impurities. It is shown that the presence of Cr atoms reduces the diffusivity of SIAs and their clusters in a non monotonic way with increasing Cr concentration. The main reason for this reduction is the presence of a long-range attractive interaction between self-interstitials in the crowdion configuration and Cr atoms. The migration mechanisms behind this effect are discussed relying on the results obtained from the MD simulations.

Table of contents

1. Introduction	6
2. Computational details and theoretical background	8
2.1 Interatomic potential and static calculations	8
2.2 Molecular dynamics simulations	10
2.3 Diffusion coefficient calculations	11
2.4 Phenomenological coefficients	14
3. Results	15
3.1 Single interstitial	15
3.2 SIA clusters	21
3.2.1 <i>Static calculations</i>	21
3.2.2 <i>Dynamic calculations</i>	22
4. Discussion	30
5. Summary, conclusions and outlook	32
Acknowledgements	32
References	32

1. Introduction

Simulations of displacement cascades performed during the last decade using molecular dynamics (MD) have clearly revealed that the primary damage state is characterised in α -Fe [1-9], as well as in other pure metals, such as Cu [2,10-13], by the formation of clusters of both self-interstitial atoms (SIA) and vacancies. The presence of a high concentration of solute atoms, such as Cr atoms in α -Fe, does not change this result [7,14,15]. A large body of literature devoted to the study of the stability and mobility of SIA clusters in pure elements such as α -Fe and Cu exists already [16-27]. These studies globally show that SIA clusters in α -Fe are collections of $\langle 111 \rangle$ crowdions which are also describable as $\frac{1}{2}\langle 111 \rangle$ loops above a certain size. These clusters exhibit high thermal stability and move one-dimensionally (1D), at least within the timescale accessible to MD; only the very small ones (di- and tri-interstitials) undergo occasional changes of glide direction, thereby approaching an overall three-dimensional (3D) motion. The activation energy for 1D glide is very low, namely a few tens of meV, and this high mobility is observed even in loops containing as many as 91 SIA.

In the case of concentrated Fe-Cr alloys, MD simulations of displacement cascades [7,14,15], supported by ab initio studies [28], have clearly shown that a strong association exists between single-interstitial or interstitial clusters and solute atoms. In particular, a large number of isolated Fe-Cr dumbbells is formed and clusters appear to contain a concentration of Cr atoms invariably larger than the alloy concentration [7,14,15]. The latter result is consistent with the experimental observation of Cr enrichment at the edge of large dislocation loops of interstitial type in electron irradiated Fe-10%Cr alloys [29]. The question addressed in the present work is how this situation will influence the mobility of interstitials and interstitial clusters in concentrated Fe-Cr alloys of different compositions.

The studies so far performed on SIA cluster stability and mobility in metals do not encompass the effect of the presence of alloying elements, with only few exceptions in the case of diluted Fe-Cu alloys [26]. Theoretical evaluations and kinetic Monte Carlo simulations suggest that solute atoms can significantly reduce and influence the diffusivity of interstitial loops [30, 31]. In particular, recent experiments on irradiated Fe-Cr alloys show that high concentrations ($\sim 9\text{at}\%$) of Cr atoms suppress the mobility of loops, due to trapping at Cr atoms segregated at their periphery [32]. Experiments also show that the addition of even small percentages (0.1at%) of Cr to ultra-pure Fe induces more frequent nucleation of small interstitial loops than in ultra-pure Fe without Cr addition [33] and that the observed loop density is enhanced in electron-irradiated Fe-10wt%Cr

at 25°C, as compared to pure Fe [29]. All these experimental observations support the idea of the existence of a strong effect of Cr atoms on the interstitial cluster population produced under irradiation.

Neutron-irradiation experiments on Fe-Cr alloys show also that adding Cr up to a concentration of 12wt% leads to a pronounced decrease in swelling compared to pure α -Fe, as well as to austenitic steels, with a complicated dependence on Cr concentration, dose and irradiation temperature [34-38]. Swelling has been theoretically rationalised, in the case of pure elements, within the rate theory model known as production bias model (PBM), which explicitly allows for the production of clusters in cascades and for the high, 1D mobility of thermally stable SIA clusters, in contrast with the very low mobility and relatively low thermal stability of vacancy clusters [39-44]. According to this model, it is the elimination of rapidly, 1D migrating SIA clusters at sinks that can lead to the accumulation of vacancies into voids at elevated temperature, thereby producing void swelling [43, 45]. In this framework, the diffusivity of interstitial clusters is an important parameter in determining the development of swelling, as it governs the rate of cluster removal from the system, as well as the formation of dislocation loop forests or their recombination with vacancies, due to reactions between different clusters. Interstitial cluster diffusivity can be reduced significantly if these defects interact with solute atoms or other lattice imperfections [30, 31, 46]. This may hence be a key factor for the understanding of the observed sensitivity of the microstructure evolution under irradiation, particularly concerning swelling, to material composition and deserves, therefore, close attention.

In this work, MD tools are used to study the effect of different concentrations of Cr solute atoms on interstitial and interstitial cluster diffusion properties in bcc Fe-Cr alloys, in comparison with pure α -Fe, using an empirical many-body potential which has been shown to be able to adequately reproduce the interaction between Cr atoms and point-defects in these alloys [47, 48, 15].

2. Computational details and theoretical background

2.1 Interatomic potential and static calculations

Details about the embedded atom method interatomic potential for Fe-Cr used in this work can be found elsewhere [47, 48, 15]. Here we shall only recall that this potential reproduces in a satisfactory way the binding energy of Cr atoms to interstitial configurations, when compared to first principle calculations [28], as summarised in Table 1. This energy represents the energy released when a Cr atom far away from the interstitial is put in the interstitial configuration. To illustrate how the potential succeeds in reproducing the attractive interaction between a crowdion and a Cr atom, in Fig. 1 we present the Fe-Fe and Fe-Cr effective pair potentials, as defined in [49]. It can be seen that, below a critical distance of $\sim 0.8 a_0$, the potential energy of an Fe-Cr pair of atoms is lower than that of an Fe-Fe pair. The interatomic separation at the centre of a crowdion in pure Fe, $\sim 0.77 a_0$, is smaller than this distance, and this is the mathematical reason for the positive binding energy between a Cr atom and a crowdion as described by the empirical potential set. The main shortcoming of the potential is that it does not provide the $\langle 110 \rangle$ dumbbell as the most stable configuration for the isolated single-interstitial. Yet, while this fact limits the validity of the results concerning single-interstitial diffusion, it does not represent a concern for the study of large enough clusters, which are known to be collections of crowdions [18-27].

Table 1. Binding energies between Cr atoms and interstitials in an Fe matrix: comparison between DFT data and empirical interatomic potential results. "Fe-Cr" denotes a mixed dumbbell, "Cr-Cr" a dumbbell containing two Cr atoms; the direction of the dumbbell is specified. Note that, in the case of the Fe-Cr $\langle 111 \rangle$ defect, the stable configuration according to the potential is actually a Cr-centered crowdion.

Binding energies (eV)	Potential	USPP-54	USPP-128	PAW-54	PAW-128
Fe-Cr $\langle 110 \rangle$	0.27	0.00	0.05	0.11	0.12
Fe-Cr $\langle 111 \rangle$	0.33	0.36	0.37	0.41	0.42
Cr-Cr $\langle 110 \rangle$	0.48	-0.55	-0.44	-0.33	-0.30
Cr-Cr $\langle 111 \rangle$	0.46	0.04	0.06	0.33	0.34

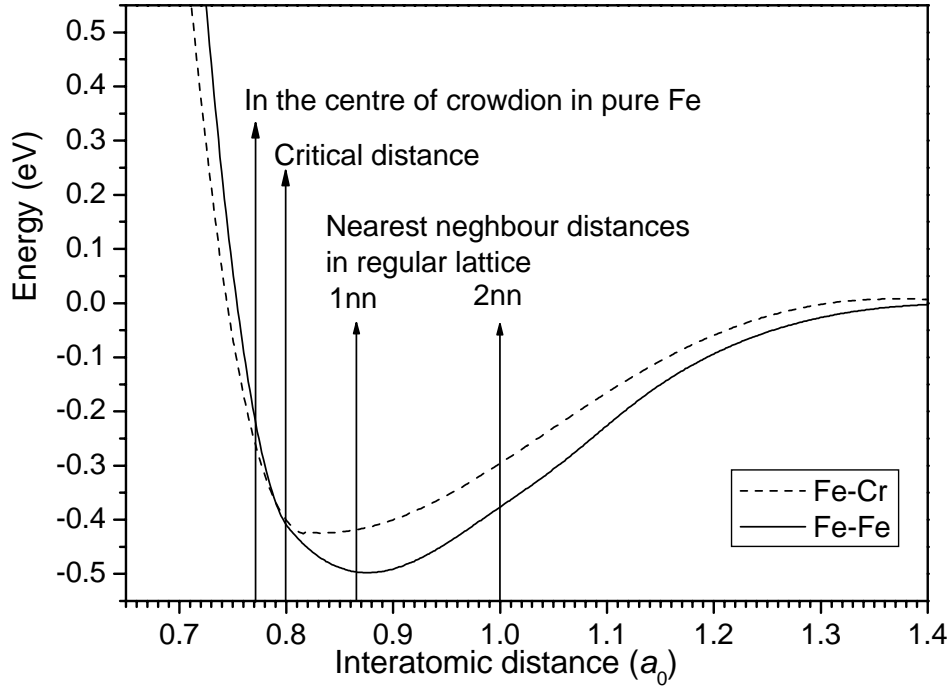


Figure 1. Fe-Fe and Fe-Cr effective pair potentials. Note the inversion of the curves above a critical distance, which explains the positive interstitial-Cr binding energy.

As a preliminary study to dynamic diffusion investigations, static calculations of formation and binding energies (E_f and E_b) for interstitial clusters associated to variable amounts of solute atoms have been performed using the present potential. These quantities have been defined in pure Fe, for a cluster of size N , as, respectively:

$$E_f(N) = (N_{sites} + N) \times [E_{MD}(\text{with cluster of size } N) - E_{coh}(\text{bcc-Fe})] \quad (1a)$$

$$E_b(N) = E_f(N) - N \times E_f(1) \quad (1b)$$

And, when N_{Cr} Cr atoms are involved:

$$E_b(N, N_{Cr}) = [E_f(N) + N_{Cr} \times E_s(\text{Cr})] - (N_{sites} + N) \times E_{MD}(\text{clus. of size } N \text{ containing } N_{Cr} \text{ Cr atoms}) \quad (2)$$

Here, N_{sites} is the size of the simulation box in terms of atomic sites, $E_{MD}(\dots)$ is the energy per atom provided by the MD code in the condition specified in parenthesis, $E_{coh}(bcc-Fe)$ is the cohesive energy of bcc-Fe and $E_s(Cr)$ is the substitution energy (heat of solution) of Cr in Fe. Note that these calculations were conducted in specimens containing only N_{Cr} atoms in an otherwise pure Fe matrix, i.e. alloying effects were not allowed for (results of calculations allowing for alloying effects were performed in [50]).

2.2 Molecular dynamics simulations

The general simulation scheme for atomic scale modelling of defect transport and features related to 1D migration have been described earlier (see i.e. [27]). In the present work cluster motion was studied using classical MD in the microcanonical (NVE) ensemble. We simulated crystals of parallelepipedic shape containing up to 120,000 atoms, applying standard periodic boundary conditions at zero pressure. Clusters of 4 to 37 SIAs in pure Fe, Fe-7at.%Cr and Fe-12at.%Cr alloys were simulated over the temperature range 300-1200 K. We also simulated single-interstitial migration in pure Fe and Fe-Cr alloys with Cr concentrations 0.2, 3, 5, 7, 9 and 12 at.%, in the same range of temperatures. All Fe-Cr substitutional alloys were prepared by uniformly and randomly distributing solute atoms in the bcc-Fe matrix.

In order to have equal statistical meaning for simulations at all temperatures, the migration process was followed for an increasing physical time (10-20 nanoseconds) with decreasing temperature, in such a way that a statistically sufficient amount of defect jumps ($N_{jump}=200-10000$) was performed in all considered cases for a given type of defect.

During the simulations interstitial atoms were identified as two atoms in the same Wigner-Seitz cell (for this reason, in what follows often the term *dumbbell* will be alternated to the term *crowdion*, in spite of the fact that, invariably, the potential used in this work predicts only the latter to be stable). Their positions were tracked together with the corresponding orientation of the interstitial configuration every few fs. The position of the cluster as a whole was defined by the coordinates of the centre of mass of the crowdions (CMC) forming the cluster. The trajectories of each crowdion, isolated or in the cluster, and of the CMCs, were thereby built and this enabled the corresponding diffusion coefficients, jump frequencies and correlation factors to be deduced, as described below (section 2.3). The jump distance was defined in all cases as equal to the first nearest neighbour distance in the bcc-Fe lattice, coincident with the Burgers vector:

$b = \frac{1}{2}\langle 111 \rangle = a_0\sqrt{3}/2 \cong 2.48 \text{ \AA}$ ($a_0 =$ lattice parameter $\cong 2.87 \text{ \AA}$). The chemical composition of the loops was also monitored.

2.3 Diffusion coefficient calculations

The dominant mode of the diffusion processes studied here is one dimensional glide and this complicates the estimation of quantitative data from atomistic modelling. General methods of treatment of MD data for the estimation of defect diffusion parameters and parameterization of simple models, particularly for the case of 1D transport, were discussed in [27]. A short description of the main methods applied here follows.

The general way to study defect diffusion by MD modelling is by monitoring the defect position and treating its temporal dependence within an appropriate atomistic model. The diffusion coefficient can thereby be obtained in terms of mean square displacement (MSD) using the well-known Einstein equation [53]. A complication comes from the restriction that usually a single and rather short (of the order of a few nanoseconds) defect trajectory is available. The way to treat this trajectory depends on the transport mechanism. In the general case, when the atomistic mechanism is unknown, the whole trajectory can be divided into smaller segments, for example of a certain time-length or consisting of a certain number of jumps. Einstein's equation can be applied and the diffusion coefficient (MSD) is then obtained as average over all segments. This technique, called here independent interval method (IIM), was first applied for single SIA diffusion in W [54] and then tested for cases of both one- and three-dimensional diffusion [27]. So, the diffusion coefficient of an N_{SIA} cluster using the IIM can be written as:

$$D_{N_{SIA}}(T) = \frac{1}{K} \sum_i^K \frac{R_i^2}{2n_d \tau_K} (T) \quad (3)$$

where, for a given temperature T , R_i is the total defect displacement in segment i of time-length $\tau_K = t_{simul}/K$, t_{simul} is the total simulation time for the specific conditions, K is the total number of segments and n_d is the dimensionality of the diffusion ($n_d = 1$ for the 1D case considered here). The time-length of the segment, τ_K , is a parameter of the model and should be long enough to include all local correlations of defect motion, i.e. should correspond to long enough trajectories. On the other side the segment cannot be very long in practice, because the statistical accuracy of the treatment is $\propto \sqrt{K}$. In the case of 1D diffusion MD simulations show that small defects at high

temperatures can change direction of motion. In this case two choices are possible for the determination of the segment time-length. Either the treatment is applied for 1D segments only, i.e. between directional changes, with $n_d=1$, thereby determining the 1D diffusion coefficient; or the three dimensional case is considered, with $n_d=3$, and in this case $\tau_K \gg \tau_{cgd}$ (where $1/\tau_{cgd}$ is the rate of directional change). Assuming that defect diffusion is a thermally activated process, its temperature dependence follows an Arrhenius law:

$$D_{N_{SIA}}(T) = D_{0,N_{SIA}} \exp\left(-\frac{E_m^{N_{SIA}}}{k_B T}\right) \quad (4)$$

where, k_B is the Boltzmann constant, $E_m^{N_{SIA}}$ is the effective activation (migration) energy and $D_{0,N_{SIA}}$ is the diffusion pre-exponential factor for the given defect.

If the defect motion can be described in terms of discrete jumps between equivalent equilibrium positions occurring at a known average rate and the jump distance is constant, as is the case for single-interstitials (position associated to the defect centre) and SIA clusters (position associated to the centre of mass), the diffusion coefficient can be written as :

$$D_{N_{SIA}}^*(T) = f_c^{N_{SIA}}(T) \frac{v^{N_{SIA}}(T) \Delta^2}{2n_d} \quad (5)$$

Here $v^{N_{SIA}}(T)$ is the SIA cluster jump frequency, $f_c^{N_{SIA}}$ is the correlation factor and Δ is the defect jump length ($\Delta = |\mathbf{b}|$ in our case, with $|\mathbf{b}| = |\frac{1}{2}\langle 111 \rangle| = \sqrt{3}/2 a_0$, a_0 being the lattice parameter). Like in eq. (3), we consider the 1D case by setting $n_d=1$ and in this instance the correlation factor is simply the ratio of forward to backward jumps[55]:

$$f_C^{N_{SIA}} = \frac{N_{for}}{N_{back}} = \frac{1 - p_r^{N_{SIA}}}{p_r^{N_{SIA}}} \quad (6)$$

where $p_r^{N_{SIA}} = N_{back}/N_{tot}$ is the probability of reversing direction for the given cluster. The method for the calculation of the 1D diffusion coefficient based on the application of eqs. (5) and (6) will be denoted as jump length method (JLM). The application of this method requires the evaluation,

from the simulation, as described above, of the jump frequency, which is the quantity of practical use in e.g. kMC simulations [56]. If the jump process is thermally activated, which is the case considered here, the temperature dependence of the jump rate, or jump frequency, of the particular SIA cluster obeys an Arrhenius law:

$$v^{N_{SIA}}(T) = v_0^{N_{SIA}} \exp\left(-\frac{E_m^{N_{SIA}}}{k_B T}\right) \quad (7)$$

where $v_0^{N_{SIA}}$ is the cluster jump attempt frequency. As was discussed in [58], the effective activation energy $E_m^{N_{SIA}}$ for a cluster can be different for the diffusion, eq.(3), and jump, eq.(7), processes. One of the reasons for this can be temperature dependence of the correlation factor, eq.(6).

Eq. (5) can be adapted also to study the case of 1D migrating defects with relatively frequent changes of direction of motion (1D/3D motion). It can indeed be demonstrated that, if a defect follows a completely isotropic random walk, i.e. in the case of a fully 3D diffusion, $f_c \rightarrow 1$ and can hence be dropped in eq. 5. The case of 1D/3D motion can be formally reduced to a 3D motion problem if the single-jump frequency of the studied SIA or SIA cluster, $v^{N_{SIA}}(T)$, is substituted with the frequency of change of glide direction of the same defect, $v_{cgd}^{N_{SIA}}(T)$, and the jump distance Δ with the average distance between changes of glide direction, Δ_{cgd} [51]. Eq. (5) transforms then, with $n_d=3$, into:

$$D_{N_{SIA}}^{d*}(T) = \frac{v_{cgd}^{N_{SIA}} \langle \Delta_{cgd}^{N_{SIA} 2} \rangle}{6} (T) = \frac{v_{cgd}^{N_{SIA}} \Delta_{fp}^{N_{SIA} 2}}{6} (T) \quad (8)$$

where $\Delta_{fp}^{N_{SIA}} \equiv \sqrt{\langle \Delta_{cgd}^{N_{SIA} 2} \rangle}$ will be denoted as defect mean free path and the related method for the calculation of the diffusion coefficient will be named free path method (FPM). In this approximate equation (the jump length is substituted by an average typical length) the analysis is switched to isotropic 3D *macrojumps*, each composed by a (variable) number of simple jumps, provided that the observation (simulation) time is long enough for the assumptions of isotropicity and randomness to hold. In this framework, an activation energy for change of direction, $E_{cgd}^{N_{SIA}}$, can be

also estimated from an Arrhenius plot versus temperature of $v_{cgd}^{N_{SIA}}$ using an equation identical to eq. (7). In addition, the scaling of the mean free path with temperature provides a criterion to assess the dimensionality of defect motion (1D versus 3D).

2.4 Phenomenological coefficients

Diffusing defects are the vehicles for solute atom transport and re-arrangement according to acting thermodynamic forces. Although generally solute atoms in alloys are assumed to move via a vacancy mechanism, under irradiation interstitials may play a role on diffusion, too. In particular, the existence of a binding energy between interstitials and Cr atoms suggests that these will actively diffuse via interstitial mechanism and it has been shown that this mechanism may in fact be more effective than the vacancy mechanism [57] and could participate in the phase transformations observed in irradiated Fe-Cr alloys [59, 60]. To understand correctly the phase transformations under irradiation, it is important to know, in particular, whether the diffusion mechanism involves fluxes with the same or opposed direction of solute atoms versus transporting defects. One way to extract this information is to look at the phenomenological coefficients, L_{ij} , as was done for example by Barashev et al. to study the possibility of dragging of P atoms in Fe by vacancies using lattice Monte Carlo simulations [61]. In order to extract the phenomenological coefficients from atomistic studies, a very convenient expression has been deduced by Allnatt [62]:

$$L_{ij} = \frac{\langle \Delta \vec{R}_i \cdot \Delta \vec{R}_j \rangle}{6Vk_B T t}, \quad i, j = \text{diffusing species} \quad (12a-9a)$$

where

$$\Delta \vec{R} = \sum_m \Delta \vec{r}_i(m) \quad (12b-9b)$$

Here, $\Delta \vec{r}_i(m)$ is the total displacement of the particle number m of type i during the observation (simulation) time t . V is the system volume, k_B is the usual Boltzmann constant and the average is taken over a canonical ensemble of systems at equilibrium. Note that $\Delta \vec{R}_i \cdot \Delta \vec{R}_j$ is a scalar product

between two displacement vectors, which will be positive if the two displacements are in the same direction and negative if they are opposite. In our case, the species of interest, i and j , are Cr and interstitial atoms and eqs. 9 have been used to study the correlation between their diffusivities.

3. Results

3.1 Single-interstitial

Before studying single-interstitial diffusion in Fe-Cr it is useful to apply first the present potential [47] to study the same problem in pure Fe, in order to have the reference case and to be aware of how it compares with previous simulation results. In Figure 2 the diffusion coefficient of the single self-interstitial atom, D^{SIA} , in Fe versus temperature is plotted as calculated by us using the IIM with different interatomic potentials [47, 63, 64] and compared with available results from the literature, where yet different potentials had been employed [4, 65, 51]. Properly commenting this figure in detail goes beyond the scope of the present report; further discussion of the figure can be found elsewhere [66]. We shall simply observe that: (i) by stabilising the easily gliding $\langle 111 \rangle$ crowdion versus the $\langle 110 \rangle$ dumbbell, the present potential overestimates, as expected, the interstitial diffusivity and predicts a trajectory made of differently orientated, consecutive $\langle 111 \rangle$ segments; yet, it gives results which are not completely out of scope, even when compared to those obtained with most available potentials featuring the correct interstitial configuration; (ii) only the potential recently fitted by Mendeleev and co-workers succeeds in providing a migration energy for the single interstitial close to the commonly accepted experimental value, around 0.25-0.3 eV [67], and a fully three-dimensional path.

Thus, Fig. 2 tells us that, when studying the single interstitial with the present potential in Fe-Cr alloys, only relative changes and trends as a function of Cr concentration will have to be retained, without trusting the absolute values. With this *caveat* in mind, in Fig. 3 the diffusion coefficient of the single interstitial in Fe-Cr alloys of different composition is plotted versus temperature and compared with the case of pure Fe.

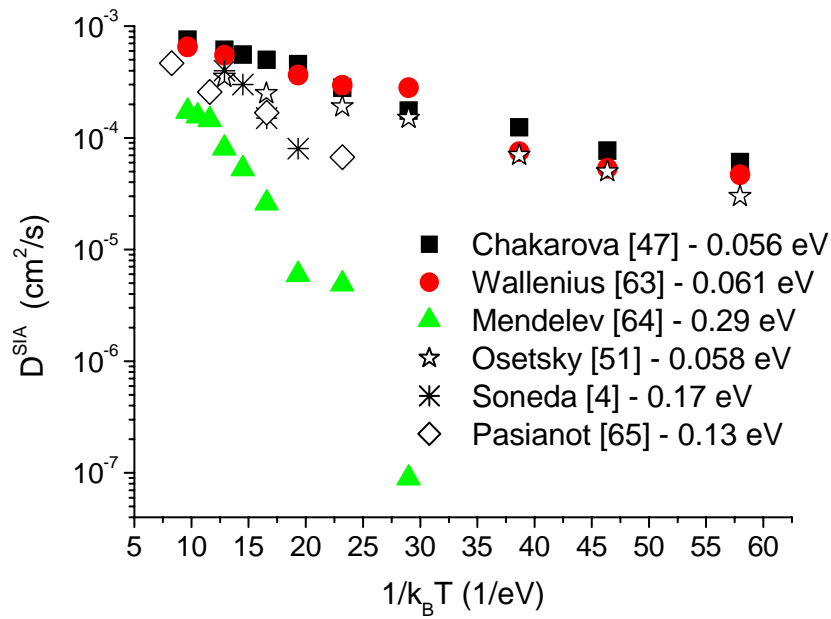


Figure 2. Diffusion coefficient of the single interstitial in pure Fe versus temperature calculated applying the IIM using different potentials. Full symbols correspond to data calculated for this work, other symbols denote data from the literature. The corresponding migration energies are indicated.

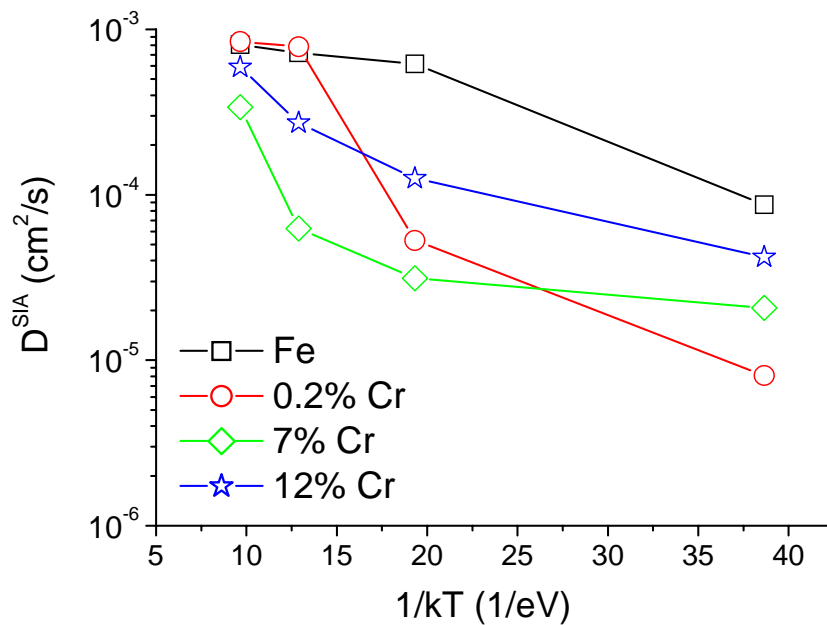


Figure 3. Diffusion coefficient of the single interstitial in Fe and Fe-Cr alloys calculated applying the IIM for different Cr concentrations.

The addition of 7% and 12% Cr atoms reduces the diffusion coefficient of the interstitial at all temperatures. Globally, by probing other concentrations, not reported on the figure, it has been found that the strongest reduction at all temperatures is obtained for 7% Cr. This point and its consequences will be further discussed in [section 4](#). The reduction of the diffusivity can be expressed as increase of the migration energy although, strictly speaking, the curves of the logarithm of D^{SIA} are not linear versus $1/k_{\text{B}}T$, thereby denoting a non-completely Arrhenius type behaviour, which limits the applicability of the concept of migration energy. This non-linear behaviour is the consequence of the transition between two regimes. At low temperature, effective trapping (binding energy of [Table 1](#)) takes place and the reduction of the diffusivity can be dramatic. In this regime, even very low Cr concentrations (e.g. 0.2%) can reduce by almost two orders of magnitude the diffusion coefficient, as compared to pure Fe. At high temperature the trapping effect is overcome and the diffusion coefficient approaches that of Fe. The transition between the two regimes, however, is clear and abrupt only for dilute alloys. In this case, the trapping mechanism can be easily visualised and understood by tracing the successive positions of the interstitial, as in [Fig. 4](#).

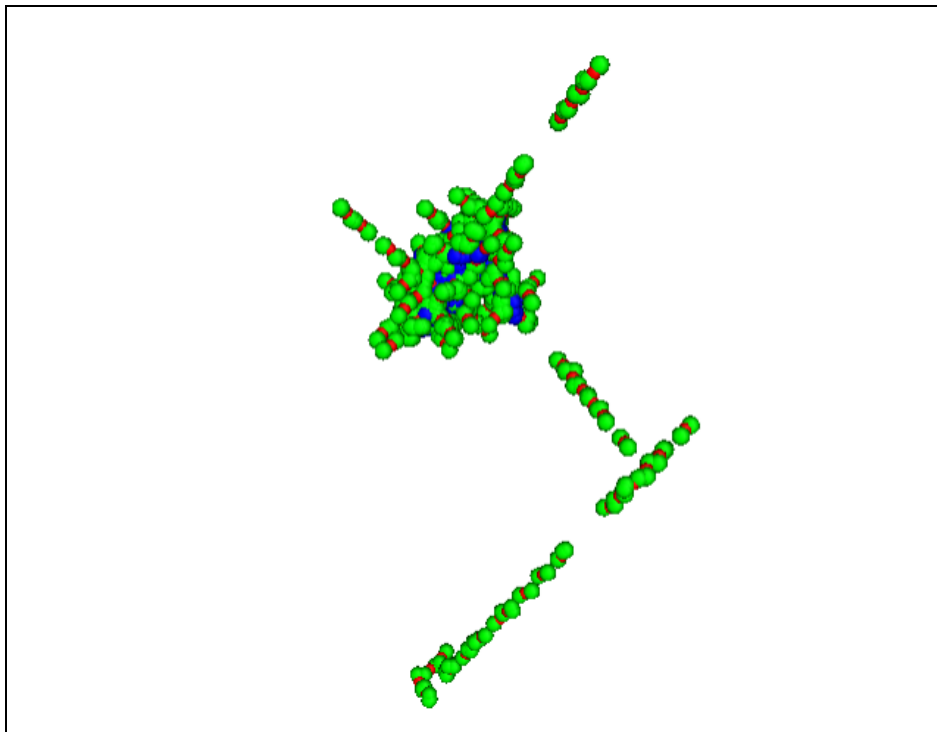


Figure 4. Pictorial representation of the successive positions of an interstitial in Fe when it encounters a Cr atom: the 1D path is deviated and the interstitial spends quite a long time around the impurity, as a consequence of the strong binding energy.

Here, light green spheres represent Fe atoms, dark blue spheres Cr atoms and small spheres (red ones) the vacant lattice site position associated to each dumbbell (since a Wigner-Seitz cell method was used to identify the interstitial, two atoms and one lattice sites are always associated to each possible interstitial configuration). It can be seen that the Fe-Fe interstitial configuration travels one-dimensionally in the material, is deviated by the presence of a Cr atom and, before leaving the Cr atom behind, spends some time describing a complicated trajectory around it. The time spent with the Cr atom will be related to the strength of the binding energy, which according to this potential (Table 1) corresponds to the 0.33 eV typical of the single-interstitial interacting with only one Cr atom in an otherwise pure Fe matrix. When the temperature is high enough to offset this binding energy, the interstitial remains essentially *transparent* to Cr atoms and the diffusion coefficient becomes the same as in pure Fe (Fig. 3).

In concentrated alloys, however, the definition of *trapping effect* is not completely unambiguous. With increasing Cr concentration the interstitial will progressively approach a situation where it can "jump" from the sphere of influence of one Cr atom to the sphere of influence of another and, at some point, interact simultaneously with more than one Cr atom, thereby lowering the net effect of the attractive interaction and counteracting the reduction of the diffusivity. Thus, the transition between the two regimes (even the *definition* of two regimes) becomes less and less sharp at higher concentrations and this qualitatively explains the non-linear temperature dependence observed in Fig. 3.

Fig. 4 suggests two general effects on the diffusion process of the crowdion in Fe which are expected to be produced by the presence of Cr: a large, temperature decreasing time spent at Cr atoms and more frequent changes of direction. This is quantified in Fig. 5 for the Fe-12%Cr alloy, where (a) the fraction of time spent as Fe-Fe, Fe-Cr and Cr-Cr configurations and (b) the mean free path (compared to the case of pure Fe) are plotted versus temperature. At all temperatures for most of the time the interstitial configuration includes at least one Cr atom and only at very high temperature the time spent far from a Cr atom becomes considerable. In the range of temperature where trapping is significant, the mean free path is strongly reduced compared to pure Fe, a sign of frequent changes of direction driven by the interaction with Cr atoms. Only above 800 K does its value become comparable with the value in pure Fe.

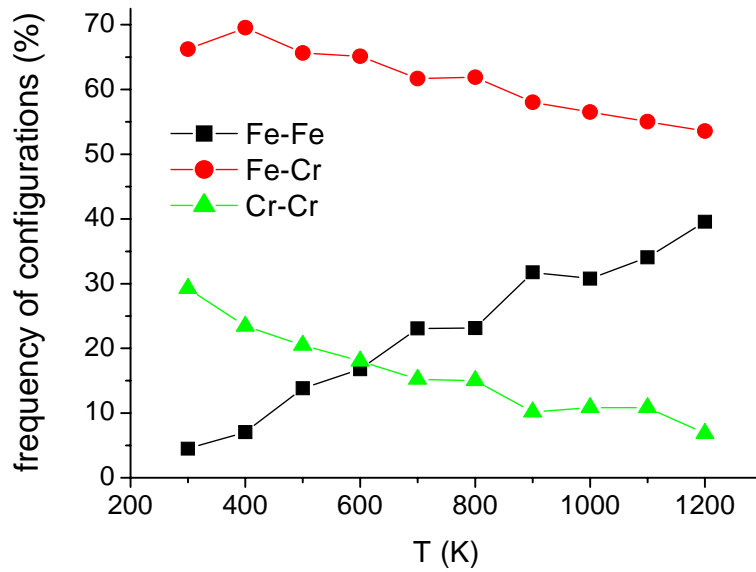


Figure 5 (a). Frequency of interstitial configurations in Fe-12%Cr versus temperature.

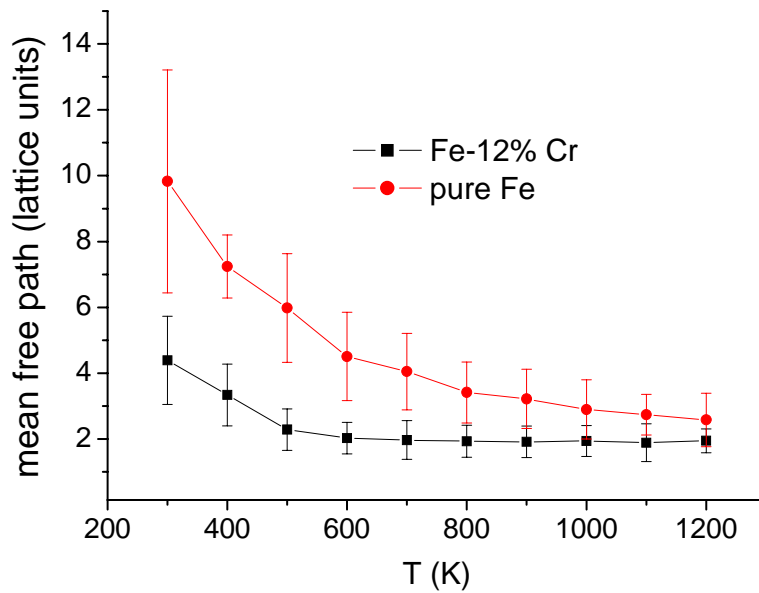


Figure 5 (b). The mean free path compared to the case of pure Fe in Fe-12%Cr versus temperature.

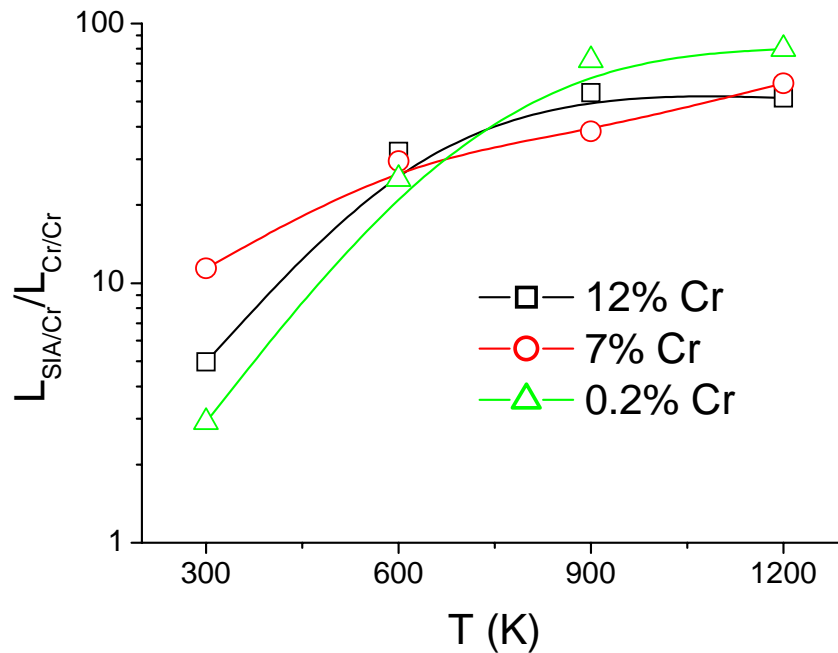


Figure 6. Ratio between phenomenological coefficients versus temperature for different Cr concentrations.

The interstitial diffusion through crowdion mechanism does not provide any means for the mixed configuration to effectively transport solute atoms without disappearing: the moment the crowdion glides, it leaves behind the atom that was at its centre. For the same reason, the moment the crowdion becomes centered at a Cr atom and subsequently leaves it behind, the net displacement of the atom will be in the same direction as the displacement of the interstitial. Thus, crowdions can contribute to solute atom diffusion, though not very effectively, and the fluxes of the two species (Cr atoms and interstitials) will be along the same direction, even in the absence of solute dragging. This is reflected by the phenomenological coefficient ratio, $L_{SIA/Cr}/L_{Cr/Cr}$, plotted in Fig. 6 versus temperature for different Cr concentrations. This ratio provides at the same time two pieces of information. Its sign informs on whether interstitials and Cr atoms move in the same direction or not. Its value is a measure of how much faster interstitials move as compared to Cr atoms. The figure shows that this ratio in the present case is always largely positive, a sign that Cr and interstitial fluxes share the same direction, but that interstitials move much faster than Cr atoms, as expected from the above reasoning on the crowdion mechanism. The lowest value is found for low temperature and relatively low Cr concentration, when effective trapping occurs (interstitials spend a long time around Cr atoms and globally both species move more or less at the same speed).

3.2 SIA Clusters

3.2.1 Static calculations

The existence of a binding energy between a single crowdion and a Cr atom explains, as outlined above, the slowing-down of single interstitial diffusion versus Cr concentration compared to pure Fe. It is therefore to be expected that it can have a role in the case of clusters, too. In order to have an idea of the potential importance of this effect, before entering the actual study of the effect of Cr on cluster motion, a set of static calculations has been performed for clusters of 3, 5, 7 and 19 crowdions, checking the influence of position and number of Cr atoms in the cluster on the magnitude of the binding energy (in an otherwise pure Fe matrix). **Fig. 7** shows the results for clusters of size 5 and 7. The binding energy appears to be broadly a linear function of the number of solute atoms in the cluster. However, for the same size, slightly different values are found, depending on how the Cr atoms were distributed inside the cluster, with stronger interaction for atoms at the periphery (recalling in this the experimental observation by Yoshida et al. [29]).

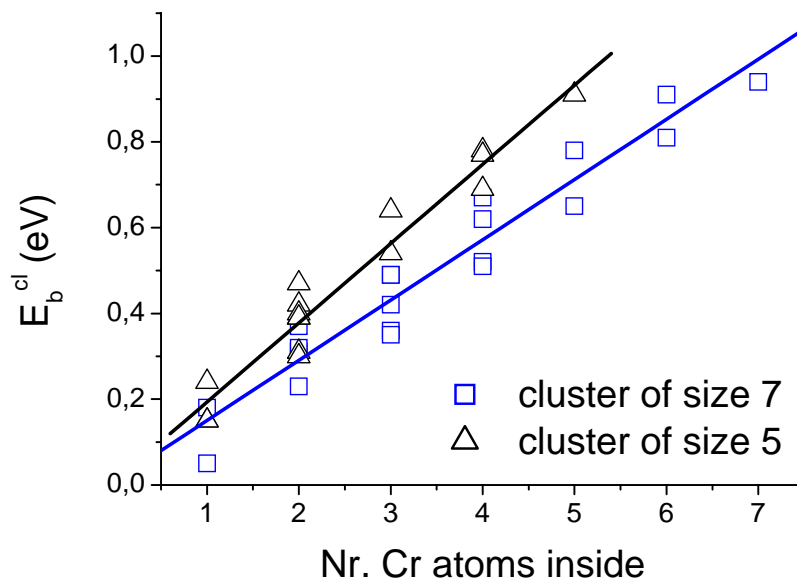


Figure 7. Binding energy of a growing number of Cr atoms to clusters of 5 and 7 interstitials.

It is interesting to observe that the partial binding energy per Cr-crowdion in cluster depends only on the cluster size, N , of which it is a decreasing function.

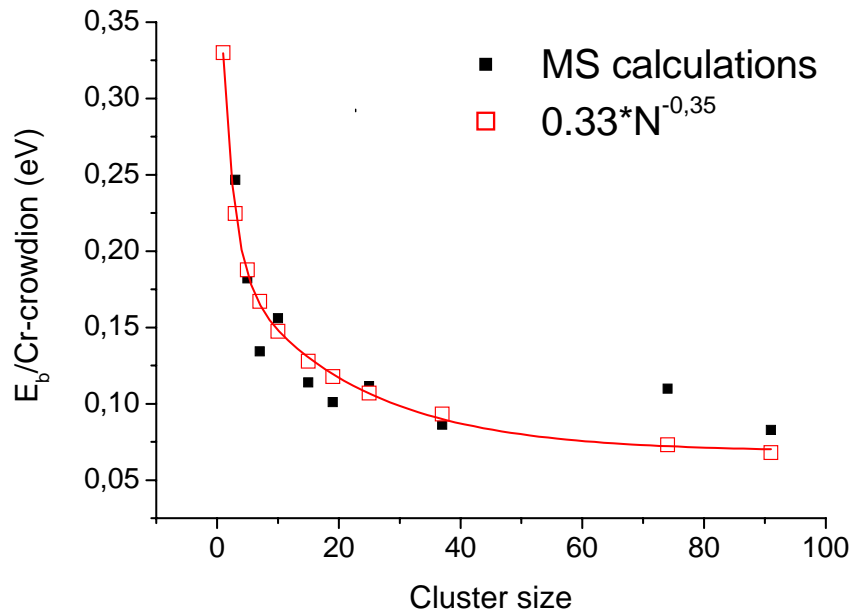


Figure 8. Binding energy per Cr-crowdion as a function of cluster size (number of interstitials).

Fig. 8 displays the points corresponding to this quantity, which can be interpolated by the function:

$$\frac{E_b^{cl}}{N} = E_b^{cd} \cdot N^{-0.35} \quad (E_b^{cl} \text{ is the binding energy of the cluster, } E_b^{cd}=0.33 \text{ eV is the binding energy of}$$

the single crowdion, see Table 1). The decrease, however, is weak enough to keep the value of the binding energy per crowdion very close to E_b^{cd} , at least for small to intermediate sizes. So, mobility reduction is indeed expected in this case, too.

3.2.2 Dynamic calculations

Fig. 9 shows the jump frequency versus temperature and size for loops in (a) pure Fe, (b) Fe-7%Cr and (c) Fe-12%Cr (data in (a) are plotted versus T_m/T , instead of $1/k_B T$, where T_m is the melting point of Fe, in order to be immediately comparable with those reported in [27]). To read the figure it should be recalled that clusters move strictly one-dimensionally along $\langle 111 \rangle$ directions within the MD timeframe, that a jump corresponds to a displacement of the centre-of-mass of the cluster equal to one Burgers vector, $b=\frac{1}{2}\langle 111 \rangle$, and that the slope of the Arrhenius plot associated to the jump frequency versus $1/k_B T$ provides by definition the migration energy, according to eq. 7.

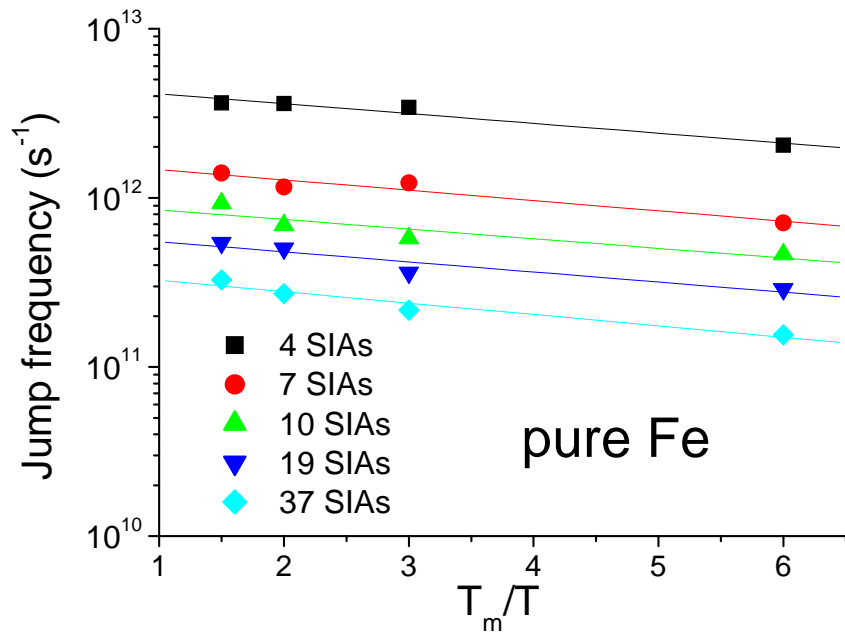


Figure 9 (a). Jump frequency versus temperature for interstitial clusters of size from 4 to 37 in pure Fe.

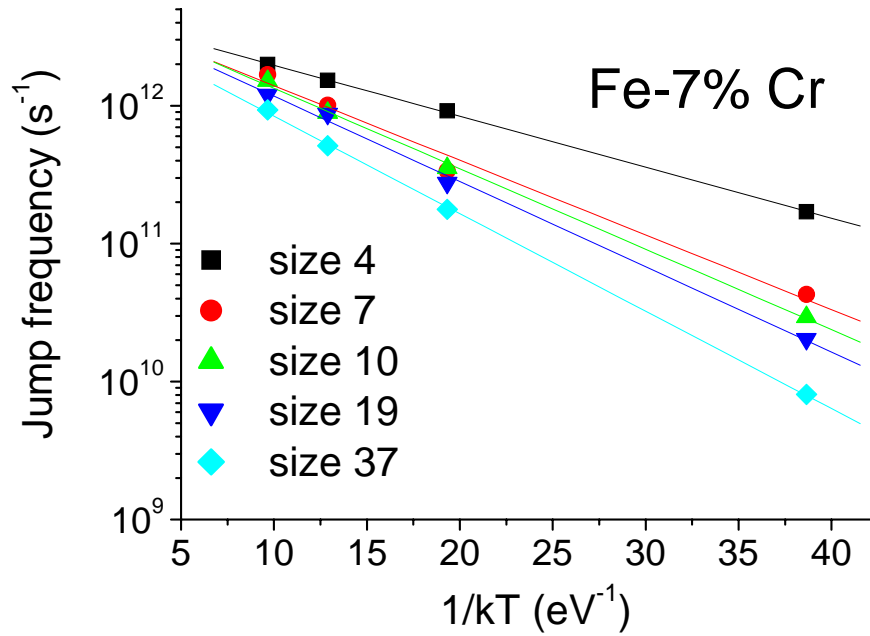


Figure 9 (a). Jump frequency versus temperature for interstitial clusters of size from 4 to 37 in Fe-7%Cr.

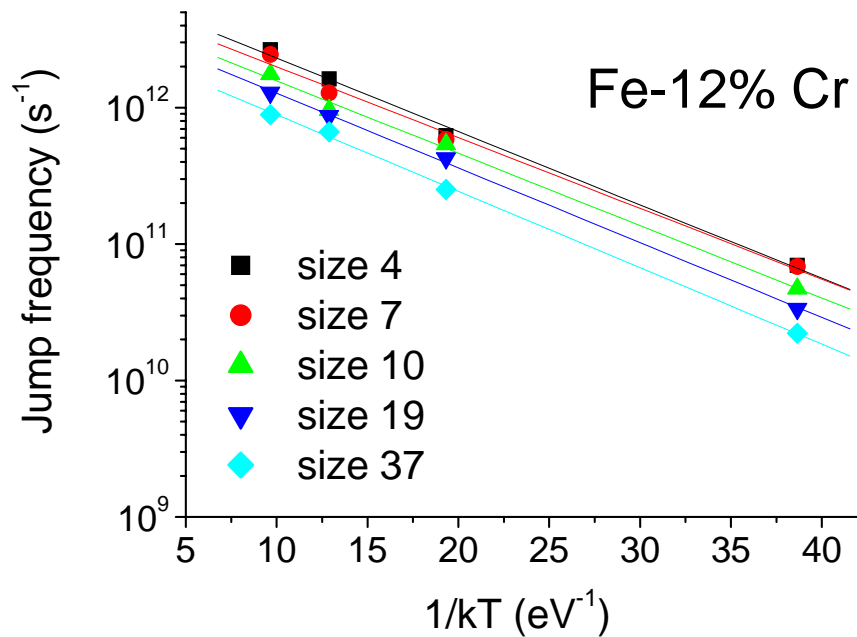


Figure 9 (a). Jump frequency versus temperature for interstitial clusters of size from 4 to 37 in Fe-12%Cr.

In pure Fe (Fig. 9a) the migration energy is found to be very low, ~ 0.02 eV, and size-independent; however, the pre-factor decreases with size. These results fully agree with those obtained for pure Fe by Osetsky and co-workers using other interatomic potentials [27, 51, 52].

In Fe-7%Cr (Fig. 9b) the migration energy becomes size-dependent and this is certainly a consequence of the fact that, in this range of concentrations, each interstitial in the cluster still interacts on average with only one Cr atom at a time and the larger the cluster, the larger the probability that an interstitial in the cluster interacts with a Cr atom, thereby increasing the overall binding energy. It is hence understandable that the migration energy should increase with size. The fact that the slope of the curves varies with size, on the other hand, causes the pre-factor to remain essentially constant.

Finally, in Fe-12%Cr (Fig. 9c) the migration energy becomes again size-independent, with a pre-factor that decreases with increasing size, like in pure Fe. The reason for this can be qualitatively understood because at high enough concentration each interstitial in the cluster will in any case be interacting with Cr atoms, possibly more than one at a time. Thus, on the one hand, the overall attractive effect will be lower (each interstitial will be able to "jump from a Cr atom to another") and, on the other, the local atomic environment around each interstitial in the cluster will

be essentially invariant and increasing the size will not increase the probability that interstitials in the cluster interact with Cr atoms. These mechanisms will be further discussed in [section 4](#).

The overall picture concerning migration energies and pre-factors is summarised in [Fig. 10](#), where these two quantities are plotted as functions of cluster size for the three cases illustrated in [Fig. 9](#).

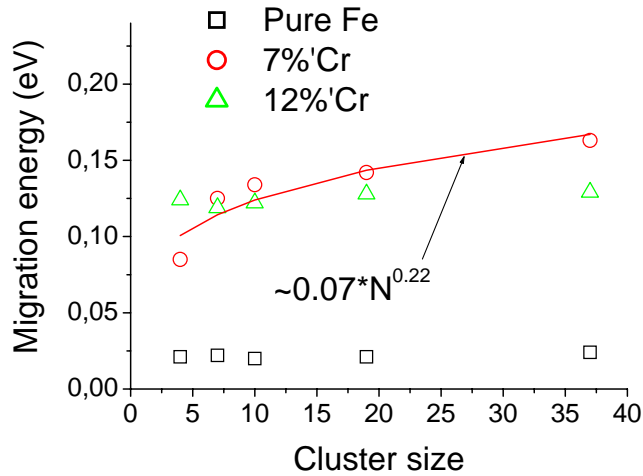


Figure 10 (a). Migration energy versus interstitial cluster size in pure Fe, Fe-7%Cr and Fe-12%Cr.

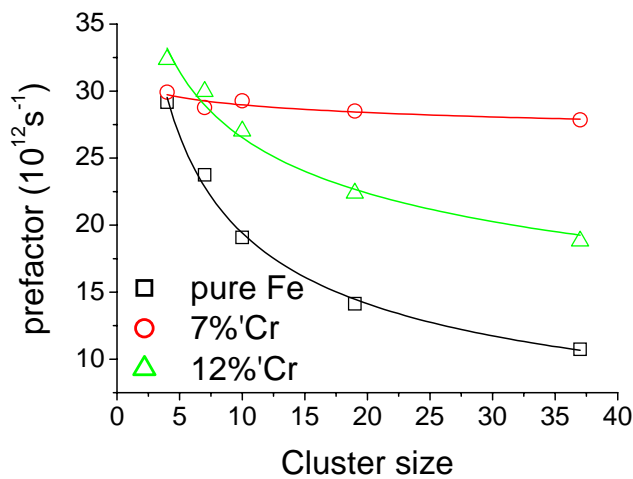


Figure 10 (b). Diffusion coefficient prefactors versus interstitial cluster size in pure Fe, Fe-7%Cr and Fe-12%Cr.

Although the migration energy is size-independent in both pure Fe and Fe-12%Cr, in the latter it is about 6 times larger (~ 0.12 eV versus ~ 0.02 eV). In Fe-7%Cr a moderate increase with size is visible and clearly for larger sizes 7%Cr provides the largest migration energy (~ 0.16 eV for size 37).

Conversely, the prefactor is essentially size-independent in this alloy, while in the case of pure Fe and Fe-12%Cr the empirical law proposed by Osetsky et al, $v_0^N = v_0 \times N^s$, can be applied. Here, v_0 is the jump frequency of the single interstitial, N is the cluster size and s is an adjustable parameter which is ~ 0.5 for pure Fe and ~ 0.25 for Fe-12%Cr.

According to eq. 5 the diffusion coefficient of the clusters is readily obtained from the jump frequency provided that the one-dimensional correlation factor, f_c^{1D} , is known (since $\Delta^2 = b^2$). The latter, in turn, can be expressed as a simple function of the probability of reversing direction of motion, p_r , using eq. 6. This probability has been measured from the simulation and, as an example, it is plotted in Fig. 11a for a cluster of size 7 in pure Fe, Fe-7%Cr and Fe-12%Cr. It is interesting to see that p_r is strongly enhanced by the presence of Cr. As a consequence of this, the distance covered by the cluster before reversing direction becomes shorter in the alloys, as illustrated in Fig. 11b, where it is shown that at 1200 K this distance is reduced on average by about 50% in Fe-12%Cr. Note that, while p_r tends to increase with temperature in pure Fe, it decreases with temperature in the alloys. Thus, at lower temperature the difference between the distance covered in pure Fe and in Fe-Cr alloys can only become larger. These data provide therefore additional insight into the mechanisms whereby Cr slows down clusters: not only the migration energy increases as a consequence of the binding to Cr atoms observed statically as well, but the slowing-down is also brought about by dynamically observed frequent changes of direction, which reduce the net displacement of the cluster. The opposite temperature behaviour of p_r compared to Fe is at any rate consistent with the fact that this effect is also related to the existence of a binding energy.

The presence of Cr not only enhances the probability of reversing direction, but also increases the probability of change of glide direction in small clusters. Fig. 12 shows the comparison between the trajectories of a 4-interstitial cluster in Fe and Fe-12%Cr at 1200 K, within the same timeframe. While in the pure element the cluster exhibits a relatively long mean free path and never changes its glide direction, in the alloy the mean free path is about an order of magnitude shorter and a change of glide direction occurs.

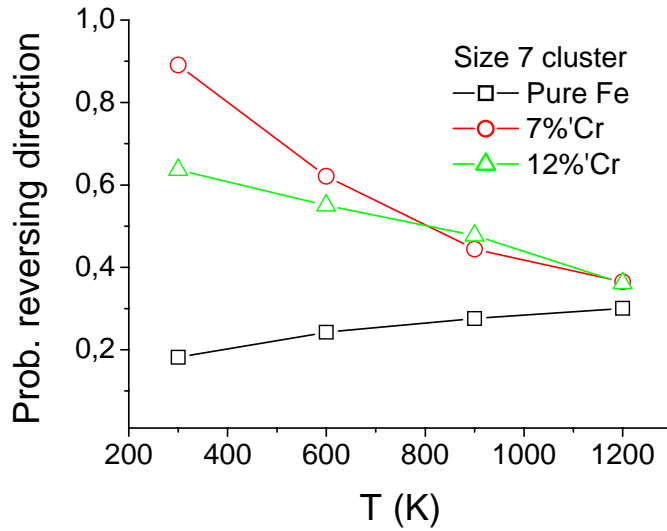


Figure 11(a). Probability of reversing direction for a 1D migrating cluster of size 7 in pure Fe, Fe-7%Cr and Fe-12%Cr versus temperature.

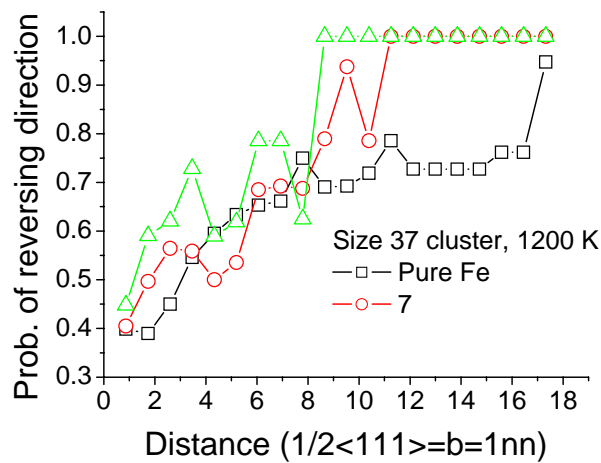


Figure 11 (b). Integral probability of reversing direction before covering a certain distance for a cluster of size 37 in pure Fe, Fe-7%Cr and Fe-12%Cr at 1200 K.

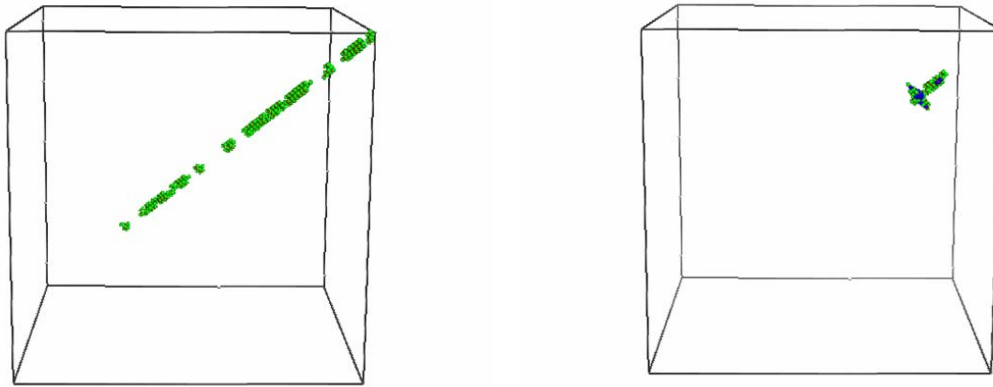


Figure 12. Comparison between the trajectory of an interstitial cluster of size 4 in pure Fe (left) and Fe-12%Cr (right) during the same amount of time at 1200 K. In Fe-Cr the cluster not only reverses its direction many times, but also succeeds in changing $\langle 111 \rangle$ glide direction.

Given the jump frequencies, shown in Fig. 9, and obtained the correlation factor via the probability of reversing direction, plotted in one specific case in Fig. 11a, all ingredients are available to obtain the diffusion coefficient of the clusters using the JLM (eq. 5). An example is given in Fig. 13, for the case of a cluster of size 37, where it appears that the migration energy is the highest in the case of 7%Cr.

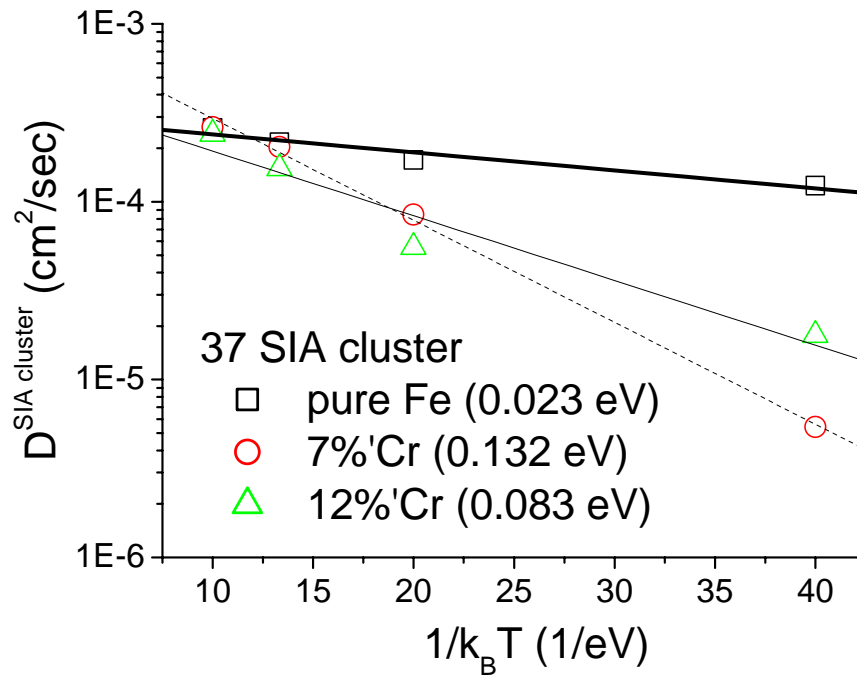


Figure 13. Diffusion coefficient versus temperature for a cluster of size 37 in Fe, Fe-7%Cr and Fe-12%Cr.

To conclude this section, we observe that a proof of the fact that the slowing down originates from the affinity between interstitials and Cr atoms comes from the measured average Cr concentration inside the clusters. As shown in Fig. 14, in both 7% and 12%Cr alloys, the percentage of Cr atoms in the clusters is always larger than the average alloy concentration, although, as is reasonable to expect, it approaches the nominal concentration for growing size.

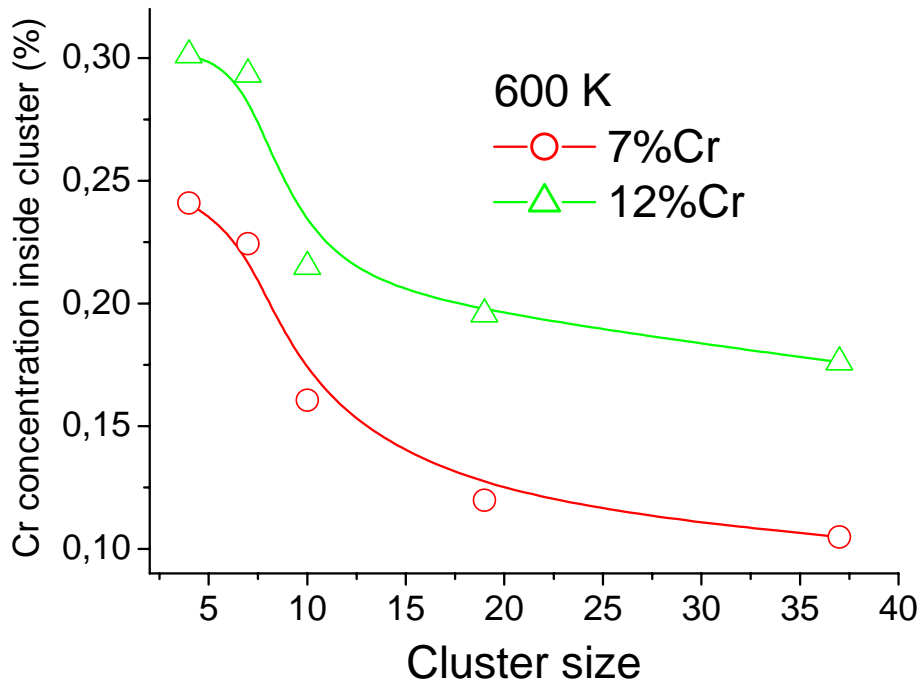


Figure 14. Average Cr concentration in interstitial clusters versus size during motion at 600 K.

The reason for this *higher-than-average* Cr concentration is two-fold: on the one hand, clusters will spend more time in regions of locally higher Cr concentration, because in those regions they become trapped; on the other, the shape of the clusters itself is distorted by the presence of Cr atoms, as the crowdions forming the clusters "look" for the closest Cr atom along their glide line, thereby maximising the number of Cr atoms involved. This is pictorially illustrated in Fig. 15 in the case of a large cluster of size 91 (static simulation), where it can be seen that clusters in Fe-Cr take a substantially different and more three-dimensional shape than in Fe, even at 0 K.

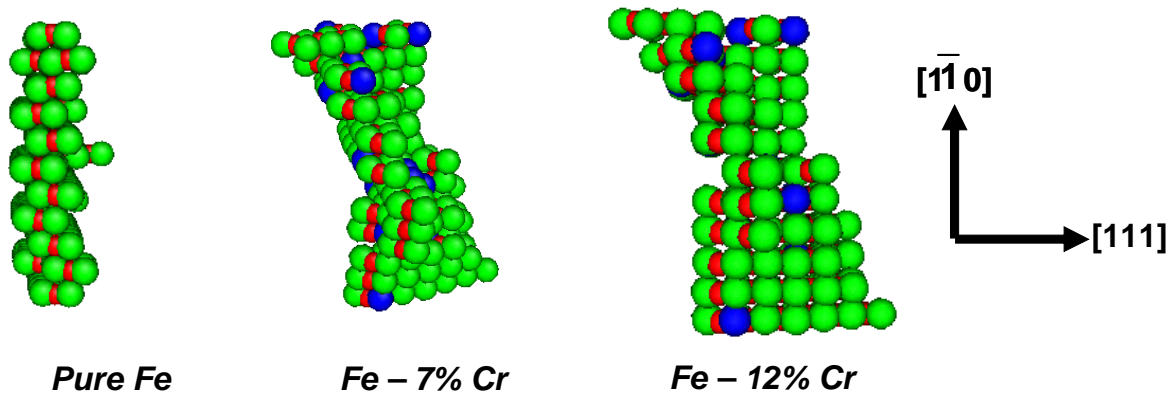


Figure 15. Pictorial representation of a cluster of 91 interstitials in pure Fe, Fe-7%Cr and Fe-12%Cr (same colour meaning as in Fig. 4).

4. Discussion

The results presented in this work suggest the following considerations:

- i. The simulation confirms the large experimental evidence for the existence of a strong interaction between Cr atoms and interstitials in Fe-Cr alloys, which produces a significant reduction of the mobility of both single-interstitial and interstitial clusters in the alloy, compared to pure Fe.
- ii. The slowing down is, however, a non-monotonic and certainly non-linear function of Cr concentration: it is most effective for intermediate concentrations ($\sim 7\%$ Cr according to the present study in the case of the single interstitial and possibly not far from such concentration for clusters of large enough size) and becomes increasingly less effective for higher concentrations, although for 12%Cr the effect remains still sensible.

These results need now to be rationalised by both elaborating a comprehensive theoretical framework and looking more in detail into the intimate physical reasons of this behaviour.

The data so far accumulated already provide good hints: the key to the problem clearly resides in the binding energy between crowdions and Cr atoms and the non-monotonic behaviour must be related to the change of the average local atomic environment of the crowdions inside the cluster with increasing Cr concentration. At low and intermediate concentrations each interstitial in the cluster, on average, will have the chance of interacting with one Cr atom at a time only. In this situation, increasing the size of the cluster will enhance the chances of a larger number of crowdions to actually interact with Cr atoms. Figs. 7 and 8 suggest that in these conditions a binding energy to Cr atom per crowdion on the order of ~ 0.1 eV can be defined and that the total

binding energy of the cluster is roughly additive, i.e. $\sim 0.1 \times N_{Cr}$ eV. Thus, in this regime increasing the size will increase the number of involved Cr atoms and the corresponding binding energy, thereby making the slowing-down more effective. This is why at 7%Cr the migration energy of clusters is size-dependent. By increasing the concentration, there will be a moment when all interstitials in the cluster, on average, will interact with one Cr atom: this will be a critical concentration, because in correspondence with this point the slowing down should be the most effective and starting from this point the dependence on size should disappear. In addition, for concentrations higher than the critical one each interstitial will have the chance of interacting with more than one Cr atom at a time. This will allow each crowdion in the cluster to "jump from one Cr atom to another", thereby reducing the overall attractive effect. Starting from the critical concentration, therefore, a less effective slowing down should be expected and this is what is found for 12%Cr. These ideas have been used to develop an analytical model capable of rationalising in a quantitative way the findings herein reported, in order to show the direct connection with swelling behaviour under irradiation as a function of Cr concentration [50].

From the point of view of the insight into the detailed physical mechanisms, the present Fe-Cr potential has the shortcoming of not being realistic enough when applied to the study of single interstitials. According to this potential the single-interstitial behaves in a very similar manner to clusters and this is known not to be the case. In addition, as already discussed in [15], the potential used in this work cannot reproduce the change of sign in the mixing enthalpy undergone by Fe-Cr alloys in the 0-15% Cr range [68], which is the thermodynamic reason for the non-monotonic behaviour of the short-range order parameter in the same concentration interval that has been measured in Fe-Cr alloys [69] and for the formation of Cr-rich α' phase formation at high enough Cr concentrations [60,61,70,71]. Thus, in order for a fully physical understanding of the detailed mechanisms of interstitial-Cr interaction to be gained, not only at the level of cluster slowing down, but also in the case of single interstitials, allowing as well for thermally and radiation-driven phase transformations in Fe-Cr alloys (α' phase formation, ordering, ...), more reliable potentials are needed. The recently proposed, advanced Fe-Cr potentials based on the two-band model approach, capable of reproducing not only the main features of point-defect interaction with Cr atoms, but also the thermodynamic behaviour of the Fe-Cr system versus concentration [72, 28], is expected to provide the possibility of going more in depth in the understanding of the behaviour of Fe-Cr alloys under irradiation.

5. Summary, conclusions and outlook

The diffusion characteristics of single interstitials and interstitial clusters in Fe-Cr alloys have been studied by molecular dynamics as functions of Cr concentration using an interatomic potential capable of adequately reproducing the interaction between point-defects and Cr atoms in Fe. In particular, this potential predicts fairly correctly the existence of an attractive interaction between interstitials in the crowdion configuration and Cr atoms, in agreement with *ab initio* calculations. The existence of this Cr-interstitial interaction provides a key to the interpretation of a large number of experimental facts, among them the reduction of the mobility and enhanced density under irradiation of interstitial clusters in Fe-Cr alloys. The present computational study has confirmed that this reduction of the mobility exists and is due to both reduced migration energy and increased probability of change of direction of motion. In addition, the present study has shown that the reduction of the interstitial cluster mobility is a non-monotonic function of Cr concentration, with a minimum around $\sim 7\%$ Cr (at least in the case of the single interstitial with the present potential). This non-monotonic behaviour in this concentration range is frequent in Fe-Cr alloys and has been observed e.g. in the case of swelling behaviour under irradiation. In a broad production bias model framework, it is legitimate to see a correlation between the non-monotonic reduction of interstitial cluster mobility and swelling behaviour. These ideas have motivated the development of an analytical model capable of rationalising the findings and considerations presented in the present paper, showing the correlation between swelling behaviour and interstitial cluster mobility in Fe-Cr alloys [50].

Acknowledgements

This work is reported for the Eurotrans IP/DEMETRA subproject. The scientific advice of A.V. Barashev and Yu.N. Osetsky in the course of the realisation of the present work is gratefully acknowledged.

References

- [1] A. F. Calder and D. J. Bacon, *J. Nucl. Mater.* **207** (1993) 25.
- [2] W. J. Phythian, A. J. E. Foreman, R. E. Stoller, D. J. Bacon and A. F. Calder, *J. Nucl. Mater.* **223** (1995) 245-26.
- [3] R.E. Stoller, G.R. Odette and B.D. Wirth, *J. Nucl. Mater.* **251** (1997) 49.

- [4] N. Soneda and T. Díaz de la Rubia, *Phil. Mag. A* **78**(5) (1998) 995.
- [5] R.E. Stoller, *J. Nucl. Mater.* **276** (2000) 22.
- [6] C. S. Becquart, C. Domain, A. Legris and J-C. van Duysen, *J. Nucl. Mater.* **280** (2000) 73.
- [7] D.A. Terentyev, L. Malerba and M. Hou, *Nucl. Instr. & Meth. B* **228** (2005) 156.
- [8] L. Malerba, *J. Nucl. Mater* **351** (2006) 28-38.
- [9] D.A. Terentyev, C. Lagerstedt, P. Olsson, K. Nordlund, J. Wallenius, C.S. Becquart and L. Malerba, *J. Nucl. Mater* 351 (2006) 65-77.
- [10] A. J. E. Foreman, W. J. Phytian and C. A. English, *Phil. Mag. A* **66** (1992) 671-695.
- [11] D.J. Bacon, A. F. Calder, F. Gao, V. G. Kapinos and S. J. Wooding, *Nucl. Instr. & Meth. B* **102** (1995) 37.
- [12] D.J. Bacon, A. F. Calder, F. Gao, *J. Nucl. Mater.* **251** (1997) 1.
- [13] D.J. Bacon, F. Gao and Yu. Osetsky, *J. Nucl Mater.* **276** (2000) 1.
- [14] L. Malerba, D.A. Terentyev, P. Olsson, R. Chakarova and J. Wallenius, *J. Nucl. Mater.* **329-333** (2004) 1156-1160.
- [15] D.A. Terentyev, L. Malerba, R. Chakarova, K. Nordlund, P. Olsson, M. Rieth and J. Wallenius, *J. Nucl. Mater.* **349** (2006) 119.
- [16] R. Bullough and R.C. Perrin, *Proc. Roy. Soc. A* **305** (1968) 541.
- [17] J.M. Harder and D.J. Bacon, *Phil. Mag. A* **58** (1988) 165.
- [18] B.D. Wirth, G.R. Odette, D. Maroudas and G.E. Lucas, *J. Nucl. Mater.* **244** (1997) 185.
- [19] Yu.N. Osetsky, M. Victoria, A. Serra, S.I. Golubov and V. Priego, *J. Nucl. Mater.* **251** (1997) 34.
- [20] Yu.N Osetsky, A. Serra and V. Priego, in: "Diffusion mechanisms in crystalline materials", Y. Mishin, G. Vogl, N. Cowen, R. Callow and D. Farkas Eds., *Mater. Res. Soc. Symp. Proc.* **527** (1998) 59.
- [21] Yu.N. Osetsky, D.J. Bacon, A. Serra, B.N. Singh and S.I. Golubov, *J. Nucl. Mater.* **276** (2000) 65.
- [22] Yu.N. Osetsky, A. Serra, B.N. Singh and S.I. Golubov, *Phil. Mag. A* **80** (2000) 2131.
- [23] B.D. Wirth, G.R. Odette, D. Maroudas and G.E. Lucas, *J. Nucl. Mater.* **276** (2000) 33.
- [24] A.V. Barashev, Yu.N. Osetsky and D.J. Bacon, *Phil. Mag. A* **80** (2000) 2709.
- [25] N. Soneda and T. Díaz de la Rubia, *Phil. Mag. A* **81** (2001) 331.
- [26] J. Marian, B.D. Wirth, A. Caro, B. Sadigh, G.R. Odette, J.M. Perlado and T. Díaz de la Rubia, *Phys. Rev. B* **65** (2002) 144102.
- [27] Yu.N. Osetsky, D.J. Bacon, A. Serra, B.N. Singh and S.I. Golubov, *Phil. Mag.* **83** (2003) 61.

- [28] Olsson, PhD dissertation: *Modelling of Formation and Evolution of Defects and Precipitates in Fe–Cr Alloys of Reactor Relevance*, U. Uppsala (Sweden), November 2005.
- [29] N. Yoshida, A. Yamaguchi, T. Muroga, Y. Miyamoto, and K. Kitajima, *J. Nucl. Mater.* **155-157** (1988) 1232.
- [30] G. A. Cottrell, S. L. Dudarev and R. A. Forrest, *J. Nucl. Mater.* **325**, 195 (2004).
- [31] T.S. Hudson, S.L. Dudarev and A.P. Sutton, *Proc. R. Soc. London A* 460 (2004) 2457.
- [32] K. Arakawa, M. Hatanaka, H. Mori, and K. Ono, *J. Nucl. Mater.* **329-333** (2004) 1194.
- [33] A. Okada, H. Maeda, K. Hamada, and I. Ishida, *J. Nucl. Mater.* **256** (1999) 247.
- [34] E.A. Little and D.A. Stow, *J. Nucl. Mater.* **87** (1979) 25.
- [35] S.I. Porollo, A.M. Dvoriashin, A.N. Vorobyev, and Yu.V. Konobeev, *J. Nucl. Mater.* **256** (1998) 247.
- [36] F.A. Garner, M.B. Toloczko and B.H. Sencer, *J. Nucl. Mater.* **276**, 123 (2000).
- [37] D.S. Gelles, *J. Nucl. Mater.* **108&109** (1982) 515.
- [38] B.H. Sencer and F.A. Garner, *J. Nucl. Mater.* **283-287** (2000) 164.
- [39] C.H. Woo and B.N. Singh, *Phys. Status Solidi (b)* **159** (1990) 609.
- [40] C.H. Woo and B. N. Singh, *Phil. Mag. A* **65** (1992) 889.
- [41] H. Trinkaus, B.N.Singh and A.J.E. Foreman, *J. Nucl. Mater.* **199** (1992) 5.
- [42] H. Trinkaus, B.N.Singh and A.J.E. Foreman, *J. Nucl. Mater.* **206** (1993) 200.
- [43] B.N. Singh, S.I. Golubov, H. Trinkaus, A. Serra, Yu.N. Osetsky, and A.V. Barashev, *J. Nucl. Mater.* **251** (1997) 107.
- [44] S.I. Golubov, B.N. Singh and H. Trinkaus, *J. Nucl. Mater.* 276 (2000) 78.
- [45] B.N. Singh, *Radiat. Eff. and Def. in Solids* **148** (1999) 383.
- [46] M. Pelfort, Yu.N. Osetsky and A. Serra, *Philos. Mag. Lett. A* **81** (2001) 803.
- [47] R. Chakarova, V. Pontikis and J. Wallenius, "Development of Fe(bcc)-Cr many body potential and cohesion model", Delivery report WP6, SPIRE project, EC contract no. FIKW-CT-2000-00058 (June 2002), available at www.neutron.kth.se/publications/library/DR-6.pdf.
- [48] P. Olsson, L. Malerba and A. Almazouzi, SCK•CEN Report, BLG-950 (June 2003).
- [49] M. S. Daw and M. I. Baskes, *Phys. Rev. B* **29**, 6443 (1984).
- [50] D.A. Terentyev, A.V. Barashev and L. Malerba, *Philos. Mag. Lett.* **85** (2005) 587.
- [51] Yu.N. Osetsky and A. Serra, *Defects and Diffusion Forum* **143-147** (1997) 155.
- [52] Yu.N Osetsky, A. Serra, V. Priego, F. Gao and D.J. Bacon, in: "Diffusion mechanisms in crystalline materials", Y. Mishin, G. Vogl, N. Cowen, R. Callow and D. Farkas Eds., *Mater. Res. Soc. Symp. Proc.* **527** (1998) 49.

- [53] A. Einstein, Ann. Phys. **17** (1905) 549.
- [54] M. W. Guinan, R. N. Stuart and R. J. Borg, Phys. Rev. B **15** (1977) 699.
- [55] J. R. Manning, *Diffusion Kinetics for Atoms in Crystals* (Van Nostrand, Toronto, 1968) p. 88.
- [56] C. Domain, C.S. Becquart and L. Malerba, J. Nucl. Mater. **335** (2004) 121.
- [57] D.A. Terentyev, L. Malerba, P. Olsson and M. Hou, in: SPIE Proceedings, A. I. Melker Editor, vol. **5400** (2004, The Society of Photo-Optical Instrumentation Engineers), ISBN 0-8194-5323-4, p. 85.
- [58] Yu.N. Osetsky, Def. & Diff. Forum **188-190**, 71 (2001).
- [59] N. P. Filippova, V. A. Shabashov and A. L. Nikolaev, Phys. Met. & Met. **90** (2000)145.
- [60] V.V. Sagaradze, I.I. Kositsyna, V.L. Arbuzov, V.A. Shabashov, and Yu.I. Filippov, Phys. Met. & Met. **92** (2001) 508.
- [61] A.V. Barashev, in: Proceedings of the 2nd International Conference on Multiscale Materials Modelling, Ed. N.M. Ghoniem, October 11-15, 2004, Los Angeles, California, USA (Mechanical & Aerospace Eng. Dept., UCLA, 2004 - ISBN 0-9762064-1-2), p. 483.
- [62] A.R. Allnatt and E.L. Allnatt, Phil. Mag. A **49** (1984) 625.
- [63] G.J. Ackland, M.I. Mendeleev, D.J. Srolovitz, S. Han and A.V. Barashev, J. Phys.: Condens. Matter **16** (2004) 1.
- [64] J. Wallenius, P. Olsson and C. Lagerstedt, Nucl. Instr. & Meth. B **228** (2005) 122.
- [65] R.C. Pasianot, A.M. Monti, G. Simonelli and E.J. Savino, J. Nucl. Mater. **276** (2000) 230-234.
- [66] D.A. Terentyev, L. Malerba and M. Hou, in: "On the dimensionality of interstitial clusters motion in bcc Fe", submitted to Phys. Rev. B.
- [67] S. Takaki, J. Fuss, H. Kugler, U. Dedek and H. Schultz, Rad. Eff. **79**, 87 (1983).
- [68] P. Olsson, I. A. Abrikosov, L. Vitos and J. Wallenius, J. Nucl. Mater. **321** (2003) 84.
- [69] I. Mirebeau, M. Hennion and G. Parette, Phys. Rev. Lett. **53** (1984) 687.
- [70] M.H. Mathon, Y. de Carlan, G. Geoffroy, X. Averty, *et al.*, J. Nucl. Mater. **312** (2003) 236.
- [71] P. Dubuisson, D. Gilbon and J.L. Séran, J. Nucl. Mater. **205** (1993) 178-189.
- [72] P. Olsson, J. Wallenius, C. Domain, K. Nordlund and L. Malerba, Phys. Rev. B. **72** (2005) 214119.